www.acsmaterialsletters.org

# Hydrogen-Bond-Promoted Planar Conformation, Crystallinity, and Charge Transport in Semiconducting Diazaisoindigo Derivatives

Published as part of "Organic Functional Materials: Special Issue in Honor of Professor Daoben Zhu on His 80th Birthday".

Anthony U. Mu, Yeon-Ju Kim, Octavio Miranda, Mariela Vazquez, Joseph Strzalka, Jie Xu, and Lei Fang\*



Downloaded via TEXAS A&M UNIV COLG STATION on June 3, 2022 at 14:49:15 (UTC). See https://pubs.acs.org/sharingguidelines for options on how to legitimately share published articles.

**Cite This:** ACS Materials Lett. 2022, 4, 1270–1278



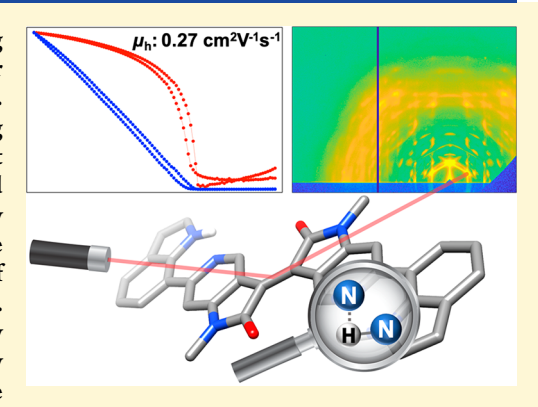
ACCESS |

Metrics & More

Article Recommendations

Supporting Information

ABSTRACT: Conformational control of  $\pi$ -conjugated molecules using intramolecular noncovalent bonds represents a promising strategy to tailor the solid-state molecular packing and electronic properties of these materials. Here, we report the design and synthesis of two model compounds featuring intramolecular hydrogen bonds formed between a center diazaisoindigo unit (the acceptor) and flanking indole units (the donor). Computational and experimental investigations show that these hydrogen bonds enthalpically stabilize the coplanar molecular conformation by >10 kcal/mol. The formation of these hydrogen bonds is also slightly favorable in terms of entropy, ensuring the high-temperature stability of the planar conformation. Thermal annealing of thin films of these compounds imparts high crystallinity and orientation in the solid state, while the non-hydrogen bond control only gave an amorphous solid. Field-effect transistor devices fabricated from these thin films exhibit hole mobilities up to 0.270 cm² V<sup>-1</sup> s<sup>-1</sup>, in contrast to the



lack of measurable charge carrier mobility for the non-hydrogen bond control. This work demonstrates an efficient synthetic strategy to incorporate robust intramolecular hydrogen bonds into conjugated  $\pi$ -systems and elucidates the mechanism on how such hydrogen bonds promote the desired molecular conformation, solid-state packing, and electronic performances of conjugated organic materials.

 $\P$  he molecular conformation of conjugated  $\pi$ -systems plays a pivotal role in governing a wide range of their properties, including solubility, solid-state characteristics, as well as optical and electronic functions. Generally, coplanar  $\pi$ -conjugated molecules are expected to possess moreextended coherent conjugation, giving rise to faster intramolecular charge transport<sup>2</sup> and lower band gaps.<sup>3</sup> A rigid coplanar conformation also favors low reorganizational energy of charge transport and close intermolecular packing in the solid state, which are anticipated to result in strong intermolecular electronic coupling and long exciton diffusion lengths. Coplanar conformations of extended  $\pi$ -systems are often accomplished by covalently fusing aromatic rings in a bottom-up manner. 2,6-8 However, extensive employment of this strategy has been limited due to challenges with precise synthesis and solution processability.

In contrast to covalent fusing, the use of dynamic noncovalent bonds can also confine the backbone conformation of conjugated molecules, <sup>10,11</sup> while potentially mitigating the aforementioned issues in synthesis and solubility. Various types of noncovalent interactions have been investigated for this purpose. For example, the installation of intrachain heteroatom interactions (e.g., S–O, S–S, S–N, S–F, S–Cl, and P–O interactions)<sup>12–19</sup> often leads to higher performances in solid-state charge transport and photovoltaics of

Received: February 22, 2022 Accepted: May 2, 2022



Scheme 1. Synthetic Route of (a) Diazaisoindigo Starting Materials and (b) the Final Products ID-C, o-AID, and p-AID

conjugated systems. However, these interactions are typically very weak (usually <1.0 kcal/mol) so that the locked coplanar conformation can easily be disrupted by thermal energy. Stronger intramolecular hydrogen bonds (H-bonds) have also been used to lock the conformation of  $\pi$ -conjugated molecular systems. For the typical C-H···F, 20,21 C-H···O, 22,23 N-H··· O, 24,25 and N-H···N<sup>26</sup> interactions, the H-bond-induced stabilizations of coplanar conformations are in the range of 7–14 kcal/mol. Many literature examples exhibited intriguing properties induced by the coplanar conformation, such as anisotropic molecular aggregation,<sup>24</sup> solvent resistance,<sup>25</sup> and increased charge carrier mobility. 21,22,26,27 Despite the potential of the H-bond approach, efficient synthetic strategies to incorporate robust intramolecular H-bonds into conjugated  $\pi$ -systems are still relatively limited. Moreover, the thermodynamic nature of intramolecular H-bonds in these  $\pi$ -systems and the mechanism on how they impact the solid-state properties are still unclear. Herein, we report a new strategy to incorporate intramolecular H-bonds into conjugated  $\pi$ -systems by utilizing diazaisoindigo acceptors; and demonstrate the crucial role of noncovalent conformational control on enhanced coplanar molecular conformation, solid-state pack-

ing, and charge-transport abilities of semiconducting organic materials

Compounds *N,N'*-bis(2-octyldodecyl)-6,6'-di(1*H*-indol-7yl)-7,7'-diazaisoindigo (o-AID) and N,N'-bis(2-octyldodecyl)-6,6'-di(1H-indol-7-yl)-5,5'-diazaisoindigo (p-AID) were designed as the models for this work. In these molecules, we employed a design<sup>28</sup> of H-bond "donor-acceptor-donor" systems, with indole as the flanking H-bond donor units and nitrogen-containing diazaisoindigo units as the H-bond acceptor in the center.<sup>29,30</sup> The central moieties in o-AID and p-AID (7,7'-diazaisoindigo<sup>31</sup> and 5,5'-diazaisoindigo,<sup>32</sup> respectively) were selected because of (i) their promising optoelectronic properties and (ii) their ability to form strainfree, favorable six-membered ring H-bonds<sup>33,34</sup> with indole. We also designed a non-H-bonded control compound N,N'bis(2-octyldodecyl)-6,6'-di(1H-indol-7-yl)-isoindigo (ID-C), which had a very similar constitution, compared to o-AID and p-AID, except for its non-nitrogen-containing center unit. ID-C did not possess a H-bond accepting unit, so it lacked any intramolecular conformational locking effect. On all of these molecules, branched alkyl chains were installed on the N-

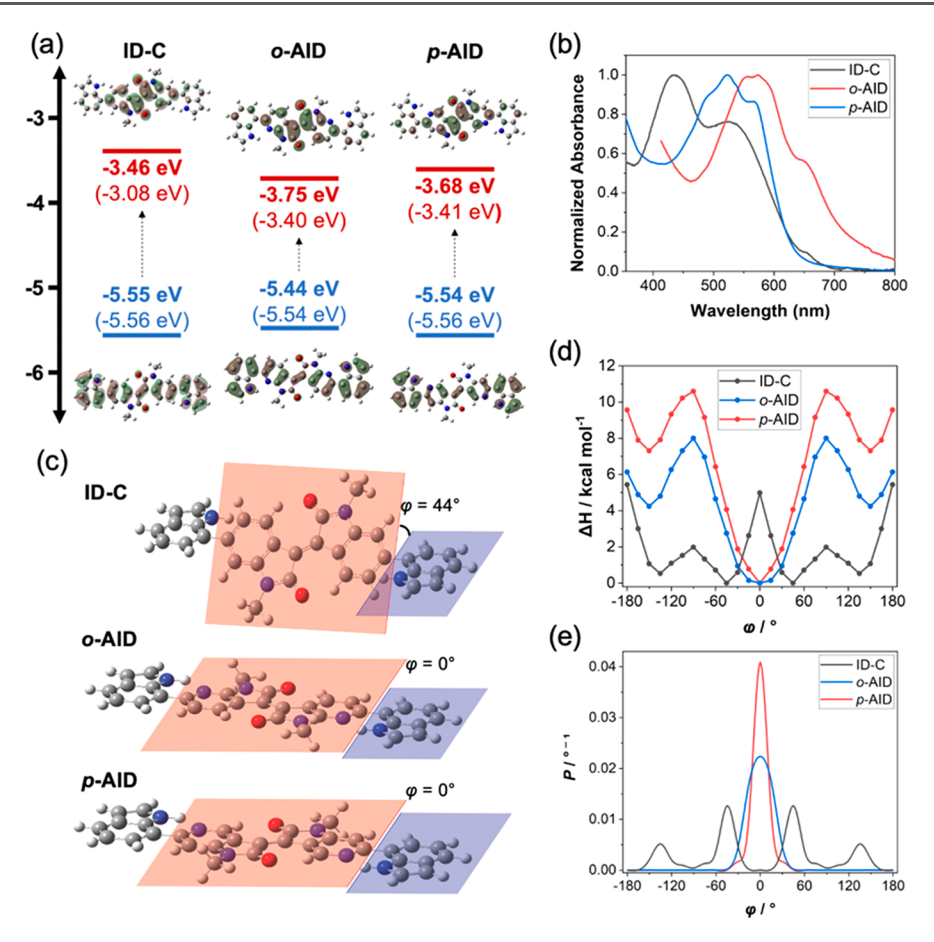


Figure 1. Optoelectronic properties and rotational energies of ID-C, o-AID, and p-AID: (a) density functional theory (DFT)-calculated frontier molecular orbital distributions of the three compounds, labeled by the corresponding energy levels obtained from CV experiments and from DFT calculation (in parentheses). (b) UV-vis spectroscopy of thin films (drop-casted on quartz glass) of ID-C, o-AID, and p-AID. (c) DFT optimized conformations of the three compounds with isoindigo planes (red) and indole planes (blue) indicated to illustrate dihedral angles. (d)  $\Delta H(\varphi)$  and (e)  $P(\varphi)$  for the three compounds, as functions of the dihedral angle  $\varphi$ . Frontier molecular orbital energy levels and rotational energies were calculated at B3LYP/6-311G(d,p) and B3LYP/6-31G(d) levels of theory, respectively.

positions of the diazaisoindigo or isoindigo units to promote solubility and solution processability.

The key synthetic steps to ID-C, o-AID, and p-AID are shown in Scheme 1. The non-nitrogen isoindigo core 3a (Scheme 1b) was synthesized according to the previously reported method.<sup>35</sup> For the synthesis of diazaisoindigo intermediates 3b and 3c, modified synthetic procedures were developed based on conditions that have been reported in the literature,<sup>36</sup> with significantly improved efficiencies (Scheme 1a). First, azaindole-derived starting materials 1 and 4 were synthesized in 10-g scales (see the SI). To synthesize the 7,7'diazaisoindigo intermediate 3b, compound 1 was oxidized into 6-bromo-7-azaisatin (2) by pyridinium chlorochromate with excess AlCl<sub>3</sub> in 62% yield. Interestingly, a small amount of 3b was already formed in this step in 27% yield, as a result of acidpromoted condensation between 1 and 2. Subsequently, in a separate batch, 2 and 1 were paired up to undergo condensation in the presence of P(NMe<sub>2</sub>)<sub>2</sub> to afford 3b. A significantly improved 53% yield in this step was achieved, compared to the literature reported 23% yield, 31 by slowly adding a solution of 2 into P(NMe<sub>2</sub>)<sub>3</sub>. The increased yield was attributed to the need of 2 equivalents of P(NMe<sub>2</sub>)<sub>3</sub> with high local concentration to drive 2 through a Kukhtin-Ramirez facilitated carbene in order to form an ylide. Subsequently, additional equivalents of 2 underwent a Wittig reaction with

the ylide to form 3b (see Scheme S1 in the Supporting Information).<sup>37,38</sup> As a result, the total yield of 3b from 1 was doubled from the literature reports of  $\sim 30\%^{31,32}$  to 60% here. Similarly, the 5,5'-diazaisoindigo core 3c was synthesized by modifying a reported method.<sup>32</sup> First, both intermediates 5 and 6 were synthesized from dibromo-functionalized starting material 4 in parallel by treating 4 with zinc or silver nitrate, respectively (details given in the SI). Purified sample 5 was then immediately condensed with 6 in an acidic condition to afford 3c in 90% yield. The yield was optimized by proceeding directly after the purification of 5 and 6 and degassing the reaction mixture to prevent the compounds from undergoing decomposition. Our modified synthesis of both 3b and 3c provided a more cost-effective approach to these diazaisoindigo-derived intermediates. Finally, Suzuki coupling between 3a, 3b, or 3c and boronic ester-functionalized indole 7 afforded the desired products ID-C, o-AID, and p-AID in yields of 83%–98%, respectively (Scheme 1b).

In order to investigate the electronic structures and energy levels of ID-C, o-AID, and p-AID, ultraviolet—visible light (UV-vis) absorption spectra (see Figure 1a, as well as Figures S11 and S12 in the Supporting Information) and cyclic voltammetry (CV) measurements were performed (Figure S14 in the Supporting Information). The observed optical bandgaps and electrochemical bandgaps were in good

agreement (see Figures 1a and 1b). According to the reduction potentials, the lowest occupied molecular orbital (LUMO) level of o-AID and p-AID (-3.75 eV and -3.68 eV) were significantly lower than that of ID-C (-3.46 eV). However, the oxidation potentials were not as significantly impacted and all showed highest occupied molecular orbital (HOMO) levels in the range from -5.55 eV to -5.44 eV for typical *p*-type organic semiconductors.<sup>39,40</sup> According to these values, o-AID and p-AID were expected to give a p-type semiconducting behavior while the *n*-type property was anticipated to be unstable, because the LUMO was not low enough.41 The overall bandgaps of o-AID and p-AID were also smaller, compared to that of **ID-C**. Indeed, their UV-vis absorption spectra (Figure 1b) were red-shifted accordingly,  $^{32,42}$  to give  $E_{\rm g}^{\rm opt}=1.74$  eV, and 1.91 eV for *o*-**AID**, and *p*-**AID**, respectively, compared to 2.02 eV for ID-C. The decreased optical and electronic bandgaps of o-AID, and p-AID were likely originated from Hbond-promoted coplanarity and the introduction of nitrogen heteroatoms. Furthermore, the solid-state absorption spectra of o-AID and p-AID demonstrated clear vibrational peaks in contrast to the smooth bands of ID-C, indicating their higher backbone rigidity induced by the conformational locking intramolecular H-bonds.

Thermogravimetric analysis (TGA) was performed for ID-C, o-AID, and p-AID to investigate their thermal stabilities (Figure S15a in the Supporting Information). While ID-C showed thermal decomposition  $(T_d)$  with 5% weight loss at a temperatures of 226 °C, o-AID and p-AID demonstrated higher thermal stabilities of 257 °C and 316 °C, respectively. The relatively low  $T_{\rm d}$  of ID-C was attributed to the thermal instability of indole, <sup>32,42,43</sup> while the higher decomposition temperatures of o-AID and p-AID implied a stabilization effect on the labile indole units after the formation of H-bonds. Their thermal properties were investigated by differential scanning calorimetry (DSC) measurements (Figures S15b-d in the Supporting Information). While ID-C did not exhibit any characteristic peaks, o-AID and p-AID demonstrated clear melting temperatures ( $T_{\rm m}$ ) of 182 °C and 111 °C, respectively, and crystallization temperatures  $(T_c)$  of 163 °C and 65 °C, respectively.

Density functional theory (DFT) calculations were employed to evaluate the strength of the intramolecular Hbonds and their effects on molecular coplanarity of o-AID and *p*-AID. Geometry optimizations [at the B3LYP/6-311G(d,p) level of theory]<sup>36,44,45</sup> demonstrated that both molecules exhibited coplanar ground-state conformations (see Figure 1c, as well as Figure S16 in the Supporting Information), while the control compound ID-C exhibited a 44° dihedral angle between the indole and isoindigo planes in its most stable conformation. The H-bond H···N distances for o-AID and p-AID were 2.11 Å and 2.07 Å, respectively, which are significantly shorter than the sum of van der Waals radii of N and H (2.75 Å).<sup>46</sup> In addition, the six-membered ring orientation allowed a ∠N-H···N angle of 120° that was favorable for the formation of H-bonds. 47,48 This observation in combination with the exceptionally downfield-shifted N-H proton signals of over 11 ppm (see Figures S5 and S9 in the Supporting Information) indicate the presence of strong Hbonding interactions. 49,50

To further quantify the conformational energy diagram of each compound and evaluate the strength of H-bonding, geometry-restricted DFT calculations were conducted at B3LYP/6-31G(d). In this study, the (diaza)isoindigo cores

of ID-C, o-AID, p-AID were restricted, while the dihedral angle  $(\varphi)$  values between the isoindigo plane and the indole plane were varied from 0° to 180° in 15° intervals. The enthalpic energy profile  $\Delta H(\phi)$  was obtained at each dihedral angle (Figure 1d). For ID-C,  $\varphi = 0^{\circ}$  was defined at the coplanar conformation closer to its ground-state orientation. For o-AID and p-AID,  $\varphi = 0^{\circ}$  was defined at their H-bonded coplanar conformations (Figure 1c). As anticipated, the rotational barriers for o-AID (8.00 kcal/mol) and p-AID (10.60 kcal/mol) were significantly higher than that of the non-H-bonded ID-C control (4.98 kcal/mol from 45°) because of the unfavorable transition state during torsional motion, in which the intramolecular H-bonds must be broken. The increased stabilization energy for p-AID compared to o-AID also implied the stronger basicity of the para-nitrogen Hbond acceptor in p-AID. Probability functions  $P(\varphi)$  (Figure 1d) were calculated for each molecule, based on the Boltzmann distribution of each conformation from the aforementioned data, to give the planarity index  $\langle \cos^2 \varphi \rangle$  as an empirical parameter according to eq 1.5

$$\langle \cos^2 \varphi \rangle = \frac{\int_0^{2\pi} P(\varphi) \cos^2 \varphi \, d\varphi}{\int_0^{2\pi} P(\varphi) \, d\varphi}$$
(1)

The planarity index  $\langle\cos^2\varphi\rangle$  [which ranges between 0 (perpendicular) and 1 (coplanar)] represented an effective quantification method for planarization. A higher planarity index was seen on *p*-AID (0.964), compared to *o*-AID (0.927), although both molecules were considered to have a planar ground-state conformation, quantifying the more rigid nature and strong intramolecular H-bonds in *p*-AID. These values were much higher than  $\langle\cos^2\varphi\rangle=0.474$  for ID-C, as expected from its nonplanar ground state.

Entropic changes of the H-bonds in o-AID and p-AID were not expected to contribute significantly, as evidenced by the relatively small yet favorable calculated entropy of formation  $(\Delta S)$  values of +9.12 cal mol<sup>-1</sup> K<sup>-1</sup> and +2.02 cal mol<sup>-1</sup> K<sup>-1</sup>, respectively. These positive  $\Delta S$  values suggested that the intramolecular H-bonds would not dissociate at high temperatures driven by entropy. To further confirm the existence and validate the intramolecular nature of these H-bonds, thereby estimating their thermodynamic robustness, variable-temperature UV-vis experiments of o-AID and p-AID in toluene were recorded in a range from 0 °C to 110 °C. Indeed, no change was observed on these spectra, even at 110 °C (see Figure S13 in the Supporting Information). Similarly, high-temperature <sup>1</sup>H NMR in toluene-d<sub>8</sub> performed at 100 °C demonstrated no significant changes compared to that at room temperature (Figure S10 in the Supporting Information). The lack of response observed in both the UV-vis spectra and <sup>1</sup>H NMR spectra in these variable conditions ruled out the possibility of intermolecular nature of these H-bonds (either with the solvent or between molecules), validating that they are intramolecular, in correlation with the DFT calculations. Furthermore, the temperature-insensitivity of the H-bonds observed in o-AID and p-AID was similar to those of independently reported examples of small molecules and proteins. 52,53 Such high-temperature robustness is critical to the thermal stability of these compounds and corresponding materials and allows for high-temperature treatments, such as solid-state thermal annealing, of these samples without disrupting the molecular conformation.

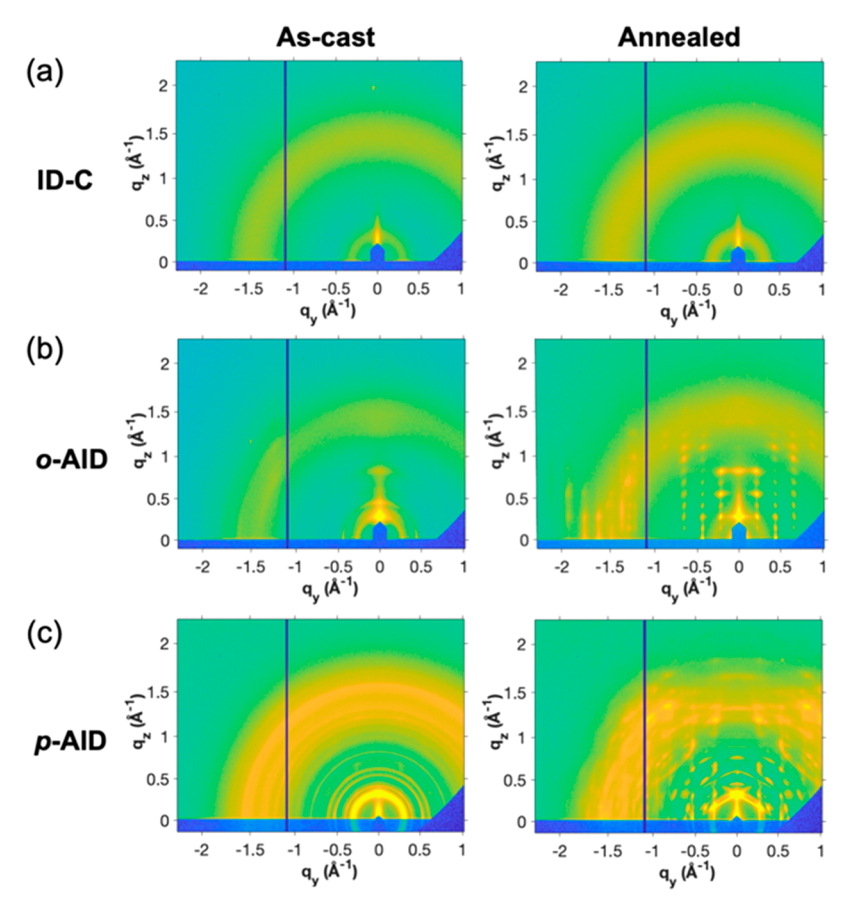


Figure 2. GIWAXS diffraction patterns for as-cast and thermally annealed thin films of (a) ID-C, (b) o-AID, and (c) p-AID.

Electrostatic potential maps calculated from the DFT optimizations were used to provide insight into potential intermolecular interactions in the solid state. p-AID demonstrated an enhanced quadrupole moment in comparison to o-AID (Figure S17 in the Supporting Information), attributed to the polarizing positions of the heteroatoms of p-AID. In contrast, the effects of the pyridinic nitrogen atoms of o-AID are mitigated by their close proximity to the solubilizing chains. The electron-rich  $\pi$ -faces of p-AID were expected to lead to stronger solid-state C-H $\cdots$  $\pi$  interactions, which were expected to promote edge-to-face stacking instead of  $\pi$ - $\pi$  stacking. S4

In order to investigate the intermolecular interactions and crystallinity with regard to solid-state charge transport properties, grazing incidence wide-angle X-ray scattering (GIWAXS) was conducted on spin-casted thin films of ID-C, o-AID, and p-AID, with or without thermal annealing (Figure 2). While single-crystal growth was unsuccessful, likely due to the bulky octyldodecyl chains necessary for solubility, GIWAXS was employed to represent the molecular packing in thin-film applications. Without thermal annealing, the spincasted p-AID thin film showed clear isotropic diffraction patterns, while ID-C and o-AID were significantly less crystalline. Nevertheless, all these thin films exhibited poor orientation in the as-cast state. Based on the DSC results, these samples were then thermally treated at 100 °C for ID-C and p-AID and 170 °C for o-AID. After this thermal annealing, multiple distinct diffraction peaks were observed on the GIWAXS results of o-AID and p-AID, demonstrating high order and orientation in these samples, while ID-C retained its amorphous character. For o-AID (Figure 2b), the diffraction

pattern suggested edge-on packing (Figure S18 in the Supporting Information) with two types of  $\pi$ - $\pi$  distances of 3.51 and 3.85 Å. Similarly, for p-AID (Figure 2c, as well as Figure S19 in the Supporting Information), the distinct  $\pi - \pi$ distance peaks at ~3.95 Å indicated tilting of the molecular backbones to  $131^{\circ}/49^{\circ}$  and  $121^{\circ}/59^{\circ}$ , corresponding to  $\pi-\pi$ packing oriented along the (220) and (210) planes, respectively. This diagonal packing was in good correlation with the DFT calculated electrostatic potential maps, in which p-AID demonstrated a higher propensity to form edge-to-face packing, compared to o-AID.<sup>54</sup> In addition, these diagonal peaks are consistent with other well-known small molecules, such as DNTT<sup>55</sup> and tetrabenzoporphyrin,<sup>56</sup> that exhibit offset packing, with respect to the substrate, which potentially leads to higher charge-transfer mobilities due to diminished grainboundary effects in thin films. 57-59 The significant differences observed here on o-AID and p-AID vs ID-C can be attributed to the thermally robust and coplanar conformation of o-AID and p-AID, which are promoted by intramolecular H-bonds. Because the H-bonds were not disrupted at higher temperatures, the rigid structures could be maintained to facilitate strong intermolecular interactions and firm molecular conformations for the formation of highly crystalline thin films with thermal annealing. In contrast, the noncrystalline property of ID-C is likely a result of the low barrier molecular torsional motion, which leads to conformational disorder and weak intermolecular interactions that hinder ordered molecular packing in the solid state.

To probe the correlation of intramolecular H-bonds and thin-film crystallinity to charge transport properties, ID-C, o-

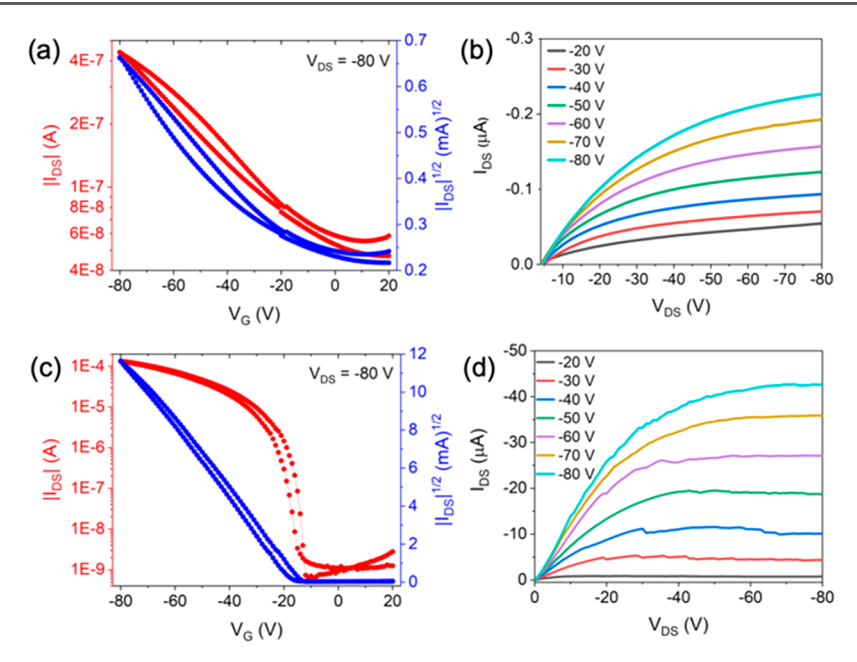


Figure 3. Transfer characteristics in the saturation regime at  $V_{\rm DS} = -80~{\rm V}$  (red) with the square root of drain current (blue) and output curves for gate voltage  $V_{\rm g} = -20~{\rm V}$  to  $-80~{\rm V}$  in 10 V increments of (a, b) o-AID and (c, d) p-AID.

AID, and p-AID were tested in the setting of organic thin-film transistors with bottom-gate/top-contact architectures. These organic materials were spin-coated onto bare or *n*-octadecyltrichlorosilane (OTS)-treated SiO<sub>2</sub>/Si substrates using Au source and drain electrodes, as detailed in the Supporting Information (SI). As-cast films of ID-C, o-AID, and p-AID showed no current modulation with the application of gate voltage, suggesting that the lack of ordered and oriented molecular packing (as indicated by GIWAXS data) is detrimental for the charge transport. Upon thermal annealing, as anticipated, the more crystalline and oriented thin films of o-AID and p-AID exhibited significantly enhanced p-type transistor performances (Figure 3). It is noteworthy that o-AID and p-AID exhibited optimized performances on different substrates, likely due to the difference in their packing modes. On the more hydrophobic OTS-modified SiO<sub>2</sub>/Si substrate, o-AID exhibited significantly increased grain boundaries with its bricklike stacking and could not form a uniform film on OTS-modified substrates. In contrast, the edge-to-face packing mode of p-AID rendered it less likely to have grain boundaries and maintained good thin film forming ability on OTSmodified substrates. After optimizing o-AID on bare SiO<sub>2</sub>/Si and p-AID on OTS-modified SiO2/Si, their maximum hole mobilities reached  $5.37 \times 10^{-4} \text{ cm}^2 \text{ V}^{-1} \text{ s}^{-1}$  and  $0.270 \text{ cm}^2 \text{ V}^{-1}$ s<sup>-1</sup>, respectively, while corresponding average hole mobilities were  $4.25 \times 10^{-4} \text{ cm}^2 \text{ V}^{-1} \text{ s}^{-1}$  and  $0.187 \text{ cm}^2 \text{ V}^{-1} \text{ s}^{-1}$  over 12 devices each. The charge transport mobilities of p-AID are higher than most of that of other small molecular isoindigoderived  $\pi$ -systems,  $^{60,61}$  and are comparable to the chargetransport mobilities of extended fused-ring isoindigo 62,63 and hemi-isoindigo derivatives. 64-66 The increased mobility of p-AID was in accordance with the favorable diagonal  $\pi$ - $\pi$ packing observed by GIWAXS. In sharp contrast, the control experiment with ID-C did not exhibit any significant fieldeffect transport (Figure S20 in the Supporting Information), even after thermal annealing, because of its lack of order in the absence of the intramolecular H-bonds.

We investigated mechanistically the impact of intramolecular H-bonds on the molecular conformation, solid-state packing, and thin-film charge transport of conjugated organic compounds. Conformation-locking intramolecular H-bonds were incorporated into diazaisoindigo-derived molecules. Facile syntheses of the key starting materials 5,5'-diazaisoindigo and 7,7'-diazaisindigo were achieved after optimizing the condensation reactions. Combined computational and experimental investigations suggested that the stabilization energy of the H-bonds promoted a high-temperature-tolerating, rigid conformation of o-AID and p-AID, in contrast to the disordered non-H-bonded control ID-C. The rigid conformation and influence of molecular design on the molecular quadrupole moment resulted in significantly enhanced orientation of solid-state molecular packing, which was clearly correlated to the semiconducting transistor performances of the thin films. Overall, this work demonstrates the effective strategy of using intramolecular H-bonds to tailor the molecular conformation, solid-state packing, and electronic properties of conjugated organic compounds.

## ASSOCIATED CONTENT

#### Supporting Information

The Supporting Information is available free of charge at https://pubs.acs.org/doi/10.1021/acsmaterialslett.2c00179.

Materials and instruments, synthetic procedures, NMR spectra, optoelectronic measurements, DSC and TGA traces, DFT calculations, grazing-incidence wide-angle X-ray scattering, transistor plots, and additional tables and figures (PDF)

#### AUTHOR INFORMATION

#### **Corresponding Author**

Lei Fang — Department of Chemistry and Department of Materials Science and Engineering, Texas A&M University, College Station, Texas 77843, United States; oocid.org/0000-0003-4757-5664; Email: fang@chem.tamu.edu

#### **Authors**

Anthony U. Mu – Department of Chemistry, Texas A&M University, College Station, Texas 77843, United States

Yeon-Ju Kim — Nanoscience and Technology Division, Argonne National Laboratory, Lemont, Illinois 60439, United States

Octavio Miranda – Department of Chemistry, Texas A&M University, College Station, Texas 77843, United States

Mariela Vazquez – Department of Chemistry, Texas A&M University, College Station, Texas 77843, United States

Joseph Strzalka — X-Ray Science Division, Argonne National Laboratory, Lemont, Illinois 60439, United States;
ocid.org/0000-0003-4619-8932

Jie Xu — Nanoscience and Technology Division, Argonne National Laboratory, Lemont, Illinois 60439, United States; o orcid.org/0000-0001-7842-5496

Complete contact information is available at: https://pubs.acs.org/10.1021/acsmaterialslett.2c00179

#### **Notes**

The authors declare no competing financial interest.

#### ACKNOWLEDGMENTS

The authors acknowledge National Science Foundation (NSF, Award No. 1654029) for financial support of this work. O.M. and M.V. acknowledge the support from NSF Graduate Research Fellowships Program. The authors acknowledge the Laboratory for Molecular Simulation at Texas A&M University for providing the Gaussian 16 software. Work performed at the Center for Nanoscale Materials and Advanced Photon Source, both U.S. Department of Energy Office of Science User Facilities, was supported by the U.S. DOE, Office of Basic Energy Sciences, under Contract No. DE-AC02-06CH11357.

### REFERENCES

- (1) Grozema, F. C.; van Duijnen, P. T.; Berlin, Y. A.; Ratner, M. A.; Siebbeles, L. D. A. Intramolecular Charge Transport along Isolated Chains of Conjugated Polymers: Effect of Torsional Disorder and Polymerization Defects. *J. Phys. Chem. B* **2002**, *106* (32), 7791–7795.
- (2) Yu, Z.-D.; Lu, Y.; Wang, J.-Y.; Pei, J. Conformation Control of Conjugated Polymers. *Chem.-Eur. J.* **2020**, 26 (69), 16194–16205.
- (3) Zhu, C.; Guo, Z.-H.; Mu, A. U.; Liu, Y.; Wheeler, S. E.; Fang, L. Low Band Gap Coplanar Conjugated Molecules Featuring Dynamic Intramolecular Lewis Acid—Base Coordination. *J. Org. Chem.* **2016**, *81* (10), 4347–4352.
- (4) Briseno, A. L.; Mannsfeld, S. C. B.; Shamberger, P. J.; Ohuchi, F. S.; Bao, Z.; Jenekhe, S. A.; Xia, Y. Self-Assembly, Molecular Packing, and Electron Transport in n-Type Polymer Semiconductor Nanobelts. *Chem. Mater.* **2008**, *20* (14), 4712–4719.
- (5) Samiullah, M.; Moghe, D.; Scherf, U.; Guha, S. Diffusion length of triplet excitons in organic semiconductors. *Phys. Rev. B* **2010**, 82 (20), 205211.
- (6) Liu, Y.; Liu, Y.; Zhan, X. High-Mobility Conjugated Polymers Based on Fused-Thiophene Building Blocks. *Macromol. Chem. Phys.* **2011**, 212 (5), 428–443.
- (7) Yang, J.; Zhao, Z.; Wang, S.; Guo, Y.; Liu, Y. Insight into High-Performance Conjugated Polymers for Organic Field-Effect Transistors. *Chem.* **2018**, *4* (12), 2748–2785.
- (8) Sun, Y.; Guo, Y.; Liu, Y. Design and synthesis of high performance  $\pi$ -conjugated materials through antiaromaticity and quinoid strategy for organic field-effect transistors. *Mater. Sci. Eng.:* R: Reports **2019**, 136, 13–26.
- (9) Lee, J.; Kalin, A. J.; Yuan, T.; Al-Hashimi, M.; Fang, L. Fully conjugated ladder polymers. *Chem. Sci.* **2017**, 8 (4), 2503–2521.

- (10) Zhu, C.; Fang, L. Locking the Coplanar Conformation of  $\pi$ -Conjugated Molecules and Macromolecules Using Dynamic Noncovalent Bonds. *Macromol. Rapid Commun.* **2018**, 39 (2), 1700241.
- (11) Mullin, W. J.; Sharber, S. A.; Thomas, S. W., III Optimizing the self-assembly of conjugated polymers and small molecules through structurally programmed non-covalent control. *J. Polym. Sci.* **2021**, *59* (15), 1643–1663.
- (12) Huang, H.; Yang, L.; Facchetti, A.; Marks, T. J. Organic and Polymeric Semiconductors Enhanced by Noncovalent Conformational Locks. *Chem. Rev.* **2017**, *117* (15), 10291–10318.
- (13) Sun, H.; Liu, B.; Koh, C. W.; Zhang, Y.; Chen, J.; Wang, Y.; Chen, P.; Tu, B.; Su, M.; Wang, H.; Tang, Y.; Shi, Y.; Woo, H. Y.; Guo, X. Imide-Functionalized Heteroarene-Based n-Type Terpolymers Incorporating Intramolecular Noncovalent Sulfur•••Oxygen Interactions for Additive-Free All-Polymer Solar Cells. *Adv. Funct. Mater.* **2019**, 29 (42), 1903970.
- (14) Li, S.; Zhao, W.; Zhang, J.; Liu, X.; Zheng, Z.; He, C.; Xu, B.; Wei, Z.; Hou, J. Influence of Covalent and Noncovalent Backbone Rigidification Strategies on the Aggregation Structures of a Wide-Band-Gap Polymer for Photovoltaic Cells. *Chem. Mater.* **2020**, 32 (5), 1993–2003.
- (15) Sinclair, G. S.; Claridge, R. C. M.; Kukor, A. J.; Hopkins, W. S.; Schipper, D. J. N-Oxide S-O chalcogen bonding in conjugated materials. *Chem. Sci.* **2021**, *12* (6), 2304–2312.
- (16) Tang, C.; Ma, X.; Wang, J.-Y.; Zhang, X.; Liao, R.; Ma, Y.; Wang, P.; Wang, P.; Wang, T.; Zhang, F.; Zheng, Q. High-Performance Ladder-Type Heteroheptacene-Based Nonfullerene Acceptors Enabled by Asymmetric Cores with Enhanced Noncovalent Intramolecular Interactions. *Angew. Chem., Int. Ed.* **2021**, *60* (35), 19314—19323.
- (17) Wang, C.-H.; Gao, Z.-C.; Sun, W.; Guo, X.; Zhang, F.-B. P···O noncovalent conformational locks for constructing highly planar Bis(diphenylphosphanyl) Bi(benzofurano). *Dyes Pigm.* **2021**, *184*, 108820.
- (18) Zhang, X.; Li, C.; Qin, L.; Chen, H.; Yu, J.; Wei, Y.; Liu, X.; Zhang, J.; Wei, Z.; Gao, F.; Peng, Q.; Huang, H. Side-Chain Engineering for Enhancing the Molecular Rigidity and Photovoltaic Performance of Noncovalently Fused-Ring Electron Acceptors. *Angew. Chem., Int. Ed.* **2021**, *60* (32), 17720–17725.
- (19) Zhang, X.; Qin, L.; Yu, J.; Li, Y.; Wei, Y.; Liu, X.; Lu, X.; Gao, F.; Huang, H. High-Performance Noncovalently Fused-Ring Electron Acceptors for Organic Solar Cells Enabled by Noncovalent Intramolecular Interactions and End-Group Engineering. *Angew. Chem., Int. Ed.* **2021**, 60 (22), 12475–12481.
- (20) Morisue, M.; Kawanishi, M.; Ueno, I.; Nakamura, T.; Nabeshima, T.; Imamura, K.; Nozaki, K. Evidence of C-F···H-C Attractive Interaction: Enforced Coplanarity of a Tetrafluorophenylene-Ethynylene-Linked Porphyrin Dimer. *J. Phys. Chem. B* **2021**, *125* (32), 9286–9295.
- (21) Wang, Y.; Hasegawa, T.; Matsumoto, H.; Michinobu, T. Significant Improvement of Unipolar n-Type Transistor Performances by Manipulating the Coplanar Backbone Conformation of Electron-Deficient Polymers via Hydrogen Bonding. *J. Am. Chem. Soc.* **2019**, 141 (8), 3566–3575.
- (22) Ocheje, M. U.; Goodman, R. B.; Lu, K.-T.; Wang, Y.; Galuska, L. A.; Soullard, L.; Cao, Z.; Zhang, S.; Yadiki, M.; Gu, X.; Chiu, Y.-C.; Rondeau-Gagné, S. Precise Control of Noncovalent Interactions in Semiconducting Polymers for High-Performance Organic Field-Effect Transistors. *Chem. Mater.* **2021**, *33*, 8267.
- (23) Lu, Y.; Yu, Z.-D.; Zhang, R.-Z.; Yao, Z.-F.; You, H.-Y.; Jiang, L.; Un, H.-I.; Dong, B.-W.; Xiong, M.; Wang, J.-Y.; Pei, J. Rigid Coplanar Polymers for Stable n-Type Polymer Thermoelectrics. *Angew. Chem., Int. Ed.* **2019**, *58* (33), 11390–11394.
- (24) Zhu, C.; Mu, A. U.; Lin, Y.-H.; Guo, Z.-H.; Yuan, T.; Wheeler, S. E.; Fang, L. Molecular Coplanarity and Self-Assembly Promoted by Intramolecular Hydrogen Bonds. *Org. Lett.* **2016**, *18* (24), 6332–6335.
- (25) Zhu, C.; Mu, A. U.; Wang, C.; Ji, X.; Fang, L. Synthesis and Solution Processing of a Rigid Polymer Enabled by Active

- Manipulation of Intramolecular Hydrogen Bonds. ACS Macro Lett. 2018, 7 (7), 801–806.
- (26) Liu, B.; Li, J.; Zeng, W.; Yang, W.; Yan, H.; Li, D.-c.; Zhou, Y.; Gao, X.; Zhang, Q. High-Performance Organic Semiconducting Polymers by a Resonance-Assisted Hydrogen Bonding Approach. *Chem. Mater.* **2021**, 33 (2), 580–588.
- (27) Wang, Q.; Böckmann, S.; Günther, F.; Streiter, M.; Zerson, M.; Scaccabarozzi, A. D.; Tan, W. L.; Komber, H.; Deibel, C.; Magerle, R.; Gemming, S.; McNeill, C. R.; Caironi, M.; Hansen, M. R.; Sommer, M. Hydrogen Bonds Control Single-Chain Conformation, Crystallinity, and Electron Transport in Isoelectronic Diketopyrrolopyrrole Copolymers. *Chem. Mater.* **2021**, 33 (7), 2635–2645.
- (28) Zhang, D.; Heeney, M. Organic Donor-Acceptor Systems. *Asian J. Org. Chem.* **2020**, 9 (9), 1251–1251.
- (29) Stalder, R.; Mei, J.; Graham, K. R.; Estrada, L. A.; Reynolds, J. R. Isoindigo, a Versatile Electron-Deficient Unit For High-Performance Organic Electronics. *Chem. Mater.* **2014**, 26 (1), 664–678.
- (30) Randell, N. M.; Kelly, T. L. Recent Advances in Isoindigo-Inspired Organic Semiconductors. *Chem. Rec.* **2019**, *19* (6), 973–988.
- (31) Huang, J.; Mao, Z.; Chen, Z.; Gao, D.; Wei, C.; Zhang, W.; Yu, G. Diazaisoindigo-Based Polymers with High-Performance Charge-Transport Properties: From Computational Screening to Experimental Characterization. *Chem. Mater.* **2016**, 28 (7), 2209–2218.
- (32) Lu, Y.; Liu, Y.; Dai, Y.-Z.; Yang, C.-Y.; Un, H.-I.; Liu, S.-W.; Shi, K.; Wang, J.-Y.; Pei, J. 5,5'-Diazaisoindigo: an Electron-Deficient Building Block for Donor—Acceptor Conjugated Polymers. *Chem. Asian J.* 2017, 12 (3), 302–307.
- (33) Kojj -Prodj, B.; Mom anov, K. The Nature of Hydrogen Bond: New Iinsights Into Old Theories. *Acta Chim. Slov.* **2008**, *55*, 692–708
- (34) Gorelik, M. V.; Gladysheva, T. K.; Shapet'ko, N. N.; Zaitsev, B. E.; Kurkovskaya, L. N.; Trankvil'nitskaya, N. A.; Mikhailova, T. A. Intramolecular hydrogen bonding with the participation of the nitrogen atom of five- and six-membered heterocycles. *Chem. Heterocycl. Compd.* 1971, 7 (2), 220–225.
- (35) Mei, J.; Graham, K. R.; Stalder, R.; Reynolds, J. R. Synthesis of Isoindigo-Based Oligothiophenes for Molecular Bulk Heterojunction Solar Cells. *Org. Lett.* **2010**, *12* (4), 660–663.
- (36) Dai, Y.-Z.; Ai, N.; Lu, Y.; Zheng, Y.-Q.; Dou, J.-H.; Shi, K.; Lei, T.; Wang, J.-Y.; Pei, J. Embedding electron-deficient nitrogen atoms in polymer backbone towards high performance n-type polymer field-effect transistors. *Chem. Sci.* **2016**, *7* (9), 5753–5757.
- (37) Zhou, R.; Zhang, K.; Chen, Y.; Meng, Q.; Liu, Y.; Li, R.; He, Z.  $P(NMe_2)_3$ -mediated reductive [1 + 4] annulation of isatins with enones: a facile synthesis of spirooxindole-dihydrofurans. *Chem. Commun.* **2015**, *51* (78), 14663–14666.
- (38) Wang, S. R.; Radosevich, A. T. P(NMe<sub>2</sub>)<sub>3</sub>-Mediated Umpolung Alkylation and Nonylidic Olefination of  $\alpha$ -Keto Esters. *Org. Lett.* **2015**, *17* (15), 3810–3813.
- (39) Cagardová, D.; Lukeš, V. Molecular orbital analysis of selected organic p-type and n-type conducting small molecules. *Acta Chimica Slovaca* **2017**, *10* (1), 6–16.
- (40) Filo, J.; Putala, M. Semiconducting Organic Molecular Materials. *J. Electr. Eng.* **2010**, *61* (5), 314–320.
- (41) Quinn, J. T. E.; Zhu, J.; Li, X.; Wang, J.; Li, Y. Recent progress in the development of n-type organic semiconductors for organic field effect transistors. *Journal of Materials Chemistry C* **2017**, 5 (34), 8654–8681.
- (42) de Miguel, G.; Camacho, L.; García-Frutos, E. M. 7,7′-Diazaisoindigo: a novel building block for organic electronics. *J. Mater. Chem. C* **2016**, *4* (6), 1208–1214.
- (43) Elsawy, W.; Lee, C.-L.; Cho, S.; Oh, S.-H.; Moon, S.-H.; Elbarbary, A.; Lee, J.-S. Isoindigo-based small molecules for high-performance solution-processed organic photovoltaic devices: the electron donating effect of the donor group on photo-physical properties and device performance. *Phys. Chem. Chem. Phys.* **2013**, *15* (36), 15193–15203.
- (44) Li, J.-L.; Chai, Y.-F.; Wang, W. V.; Shi, Z.-F.; Xu, Z.-G.; Zhang, H.-L. Pyrazine-fused isoindigo: a new building block for polymer solar

- cells with high open circuit voltage. Chem. Commun. 2017, 53 (43), 5882-5885.
- (45) Vijayan, S. M.; Sparks, N.; Roy, J. K.; Smith, C.; Tate, C.; Hammer, N. I.; Leszczynski, J.; Watkins, D. L. Evaluating Donor Effects in Isoindigo-Based Small Molecular Fluorophores. *J. Phys. Chem. A* **2020**, *124* (51), 10777–10786.
- (46) Bondi, A. van der Waals Volumes and Radii. J. Phys. Chem. 1964, 68 (3), 441–451.
- (47) Morozov, A. V.; Kortemme, T.; Tsemekhman, K.; Baker, D. Close agreement between the orientation dependence of hydrogen bonds observed in protein structures and quantum mechanical calculations. *Proc. Natl. Acad. Sci. U.S.A.* **2004**, *101* (18), 6946–6951.
- (48) Gellman, S. H.; Dado, G. P.; Liang, G. B.; Adams, B. R. Conformation-directing effects of a single intramolecular amide-amide hydrogen bond: variable-temperature NMR and IR studies on a homologous diamide series. *J. Am. Chem. Soc.* **1991**, *113* (4), 1164–1173
- (49) Dhanishta, P.; Sai Siva kumar, P.; Mishra, S. K.; Suryaprakash, N. Intramolecular hydrogen bond directed stable conformations of benzoyl phenyl oxalamides: unambiguous evidence from extensive NMR studies and DFT-based computations. *RSC Adv.* **2018**, 8 (20), 11230–11240.
- (50) Scheiner, S. Assessment of the Presence and Strength of H-Bonds by Means of Corrected NMR. *Molecules* **2016**, *21* (11), 1426.
- (51) Che, Y.; Perepichka, D. F. Quantifying Planarity in the Design of Organic Electronic Materials. *Angew. Chem., Int. Ed.* **2021**, *60* (3), 1364–1373.
- (52) Bastida, A.; Zúñiga, J.; Requena, A.; Miguel, B.; Cerezo, J. On the Role of Entropy in the Stabilization of  $\alpha$ -Helices. *J. Chem. Inf. Model.* **2020**, *60* (12), 6523–6531.
- (53) Exarchou, V.; Troganis, A.; Gerothanassis, I. P.; Tsimidou, M.; Boskou, D. Do strong intramolecular hydrogen bonds persist in aqueous solution? Variable temperature gradient <sup>1</sup>H, <sup>1</sup>H-<sup>13</sup>C GE-HSQC and GE-HMBC NMR studies of flavonols and flavones in organic and aqueous mixtures. *Tetrahedron* **2002**, *58* (37), 7423–7429.
- (54) Lin, P.-P.; Qin, G.-Y.; Zhang, N.-X.; Fan, J.-X.; Hao, X.-L.; Zou, L.-Y.; Ren, A.-M. The roles of heteroatoms and substituents on the molecular packing motif from herringbone to  $\pi$ -stacking: A theoretical study on electronic structures and intermolecular interaction of pentacene derivatives. *Org. Electron.* **2020**, *78*, 105606.
- (55) Zhou, Z.; Wu, Q.; Wang, S.; Huang, Y.-T.; Guo, H.; Feng, S.-P.; Chan, P. K. L. Field-Effect Transistors Based on 2D Organic Semiconductors Developed by a Hybrid Deposition Method. *Adv. Sci.* **2019**, *6* (19), 1900775.
- (56) Liman, C. D.; Choi, S.; Breiby, D. W.; Cochran, J. E.; Toney, M. F.; Kramer, E. J.; Chabinyc, M. L. Two-Dimensional GIWAXS Reveals a Transient Crystal Phase in Solution-Processed Thermally Converted Tetrabenzoporphyrin. *J. Phys. Chem. B* **2013**, *117* (46), 14557–14567.
- (57) Yamashita, Y. Organic semiconductors for organic field-effect transistors. Sci. Technol. Adv. Mater. 2009, 10 (2), 024313.
- (58) Inoue, S.; Nikaido, K.; Higashino, T.; Arai, S.; Tanaka, M.; Kumai, R.; Tsuzuki, S.; Horiuchi, S.; Sugiyama, H.; Segawa, Y.; Takaba, K.; Maki-Yonekura, S.; Yonekura, K.; Hasegawa, T. Emerging Disordered Layered-Herringbone Phase in Organic Semiconductors Unveiled by Electron Crystallography. *Chem. Mater.* **2022**, 34 (1), 72–83.
- (59) Ma, Z.; Geng, H.; Wang, D.; Shuai, Z. Influence of alkyl sidechain length on the carrier mobility in organic semiconductors: herringbone vs. pi—pi stacking. *J. Mater. Chem. C* **2016**, *4* (20), 4546—4555.
- (60) Shaker, M.; Park, B.; Lee, S.; Lee, K. Face-on oriented thermolabile Boc-isoindigo/thiophenes small molecules: From synthesis to OFET performance. *Dyes Pigm.* **2020**, *172*, 107784.
- (61) Patil, H.; Chang, J.; Gupta, A.; Bilic, A.; Wu, J.; Sonar, P.; Bhosale, S. V. Isoindigo-Based Small Molecules with Varied Donor Components for Solution-Processable Organic Field Effect Transistor Devices. *Molecules* **2015**, *20* (9), 17362–17377.

**ACS Materials Letters** Letter www.acsmaterialsletters.org

- (62) Xu, S.; Ai, N.; Zheng, J.; Zhao, N.; Lan, Z.; Wen, L.; Wang, X.; Pei, J.; Wan, X. Extended isoindigo core: synthesis and applications as solution-processable n-OFET materials in ambient conditions. RSC Adv. 2015, 5 (11), 8340-8344.
- (63) Hasegawa, T.; Ashizawa, M.; Matsumoto, H. Design and structure-property relationship of benzothienoisoindigo in organic field effect transistors. RSC Adv. 2015, 5 (75), 61035-61043.
- (64) Wu, T.; Yu, C.; Guo, Y.; Liu, H.; Yu, G.; Fang, Y.; Liu, Y. Synthesis, Structures, and Properties of Thieno[3,2-b]thiophene and Dithiophene Bridged Isoindigo Derivatives and Their Organic Fieldeffect Transistors Performance. J. Phys. Chem. C 2012, 116 (43), 22655-22662
- (65) Sun, M.; Sun, Y.; Chen, R.; Hu, Y.; Zhang, G. Small molecule semiconductors based on hemi-isoindigo and diketopyrrolopyrrole for solution-processed organic field-effect transistors. Synth. Met. 2021,
- (66) Zhang, G.; Chen, R.; Sun, Y.; Kang, B.; Sun, M.; Lu, H.; Qiu, L.; Cho, K.; Ding, Y. Improved charge transport in fused-ring bridged hemi-isoindigo-based small molecules by incorporating a thiophene unit for solution-processed organic field-effect transistors. J. Mater. Chem. C 2020, 8 (4), 1398-1404.

# **□** Recommended by ACS

cis-CC Bond and Amide Regulated Oriented Supramolecular Assembly on Two-Dimensional Atomic **Crystals** 

Hongde Yu, Dong Wang, et al.

NOVEMBER 27, 2019

THE JOURNAL OF PHYSICAL CHEMISTRY C

READ Z

**Tuning Conformational H-Bonding Arrays in** Aromatic/Alicyclic Polythiourea toward High Energy-**Storable Dielectric Material** 

Yang Feng, Shengtao Li, et al.

NOVEMBER 11, 2019

MACROMOLECULES

READ Z

Surface Self-Assembly, Film Morphology, and Charge **Transport Properties of Semiconducting Triazoloarenes** 

David L. Wisman, Steven L. Tait, et al.

APRIL 12, 2019

LANGMUIR

READ Z

**Mechanical Tuning of Aggregated States for** Conformation Control of Cyclized Binaphthyl at the **Air-Water Interface** 

Masaki Ishii, Katsuhiko Ariga, et al.

MAY 12, 2022

LANGMUIR

READ Z

Get More Suggestions >